

First Principles Study of Titanium Hydrides, TiH_n : $n = 1, 2, 3$; Energetics and Phase Transition

Shunmugam KANAGAPRABHA¹, Ratnavelu RAJESWARAPALANICHAMY^{2,*}
and Kombiah IYAKUTTI³

¹Department of Physics, Kamaraj College, Tuticorin, Tamil Nadu 628003, India

²Department of Physics, Nadar Mahajana Sangam S. Vellaichamy Nadar College, Madurai, Tamil Nadu 625019, India

³Department of Physics & Nanotechnology, SRM University, Chennai, Tamilnadu 603203, India

(* Corresponding author's e-mail: rrpcaspd2003@gmail.com)

Received: 17 October 2012, Revised: 12 December 2012, Accepted: 6 February 2014

Abstract

The electronic structure and structural phase transition of TiH_n ($n = 1, 2$ and 3) are investigated using the Tight-binding linear muffin-tin orbital (TB-LMTO) method with Local density approximation (LDA) and Atomic sphere approximation (ASA). The equilibrium geometries, the electronic band structure, and the total and partial Density of states (DOS) are obtained under various pressures, and are analyzed in comparison with the available experimental and theoretical data. It is predicted that the most stable structure of titanium hydride is a cubic structure at normal pressure. Both TiH and TiH_2 undergo a structural phase transition from a cubic to a hexagonal phase under high pressure. The stability of TiM_2H and TiMH_2 is analyzed.

Keywords: Ab initio calculations, electronic structure, phase transition

Introduction

Hydrogen is known to form compounds with many elements in the periodic table [1]. Among those, the metal hydrides are of particular interest due to their application in hydrogen storage for fuel cells [2,3]. The physical properties of metal hydrides are quite interesting from a practical point of view. For example, the density of hydrogen in metal hydrides is larger than that in liquid hydrogen [4]. Previously, the first principle calculations were studied for fluorite type dihydrides [5,6]. Most transition metals form hydrides at sufficiently high pressures of hydrogen [7]. Recently the electronic structure and magnetic properties of FeH and CoH [8] and the electronic structure, structural properties and superconductivity of nickel hydride [9] have been studied.

In this paper, the band structure, the density of states (DOS), the electronic charge distribution and the structural phase transition of Titanium hydrides under various pressures are investigated using first principles calculation. For Ti and TiH_3 , cubic (space group $Fm\bar{3}m$) and hexagonal (space group $P6_3/mmc$) are chosen as candidate structures of TiH , and for TiH_2 , cubic (space group $Fm\bar{3}m$) and tetragonal (space group $I4/mmm$) are chosen. The hydrogen storage capacity of titanium is calculated. Further, the stability of TiMH_2 and TiM_2H is analyzed.

Computational details

The Tight binding linear muffin-tin orbital (TB-LMTO) method has been used [10,11] to compute the electronic structure and the basic ground state properties of TiH , TiH_2 and TiH_3 . In the LMTO scheme, the crystal potential is approximated by a series of non-overlapping atomic-like spherical

potentials and a constant potential between the spheres. The Schrödinger equation can be solved in both the regions. These solutions are then matched at the sphere boundaries to produce muffin-tin orbitals. These muffin-tin orbitals are used to construct a basis which is energy independent, has a linear order in energy and is rapidly convergent. Each orbital must satisfy Schrödinger's differential equation in the region between the atoms. Here, the potential is flat on a scale of 1 Ry, and, since the energy range of interest begins near the point where the electron can pass between the atoms and extends upwards by about 1 Ry, it seems natural to choose orbitals which have zero kinetic energy, i.e., they satisfy the Laplace equation, in the interstitial region. In the tight-binding muffin-tin orbital, the solution of Schrödinger's equation is written as;

$$|\chi^\alpha(\epsilon)\rangle = \begin{cases} |\varphi(E)\rangle N^\alpha(E) + |J^\alpha\rangle P^\alpha(E) & r \leq w \\ |K^\alpha\rangle & r \geq w \end{cases} \quad (1)$$

where r is any distance from the centre of the muffin-tin sphere, w is the average Wigner-Seitz radius and α are dimensionless screening constants. Inside the MT sphere, the base field (or) unscreened field $|K\rangle$ is defined by;

$$|K\rangle = |\varphi(E)\rangle N^\alpha(E) + |J^\alpha\rangle P^\alpha(E). \quad (2)$$

In the interstitial region, the screened field $|k^\alpha\rangle$ is defined by;

$$|k^\alpha\rangle = |\varphi(E)\rangle N^\alpha(E) + |J^\alpha\rangle P^\alpha(E) - |J^\alpha\rangle S^\alpha \quad (3)$$

where $\varphi(E)$ is normalized to unity in its sphere such that $\langle \varphi(E) | \varphi(E) \rangle = 0$ and $\langle \varphi(E) | \varphi(E) \rangle = -1$.

J^α is the screen field radial function and S^α is the screened structure matrix. The elements of the diagonal matrices P and N are;

$$P^\alpha(E) = \frac{\langle \varphi(E), k \rangle}{\langle \varphi(E), J^\alpha \rangle} = \frac{P^0(E)}{1 - \alpha P^0(E)} \quad (4)$$

$$N^\alpha(E) = \frac{\langle J^\alpha, k \rangle}{\langle J^\alpha, \varphi(E) \rangle} = \left(\frac{w}{2}\right)^{1/2} P^0(E)^{1/2}. \quad (5)$$

The set of energy dependent MTOs $|\chi^\alpha(E)\rangle$ thus equals $|k^\alpha\rangle$ and $|k\rangle$; the linear combination $|\chi^\alpha(E)\rangle u^\alpha$, specified by a column vector u^α , is seen to be a solution of Schrödinger's equation at energy E for the MT potential if it equals the one center expansions $|\varphi(E)\rangle N^\alpha(E) u^\alpha$ in the spheres, i.e., if the set of linear homogeneous equations $[P^\alpha(E) - S^\alpha] u^\alpha = 0$ has a proper solution. This is the generalization of the so-called tail cancellation or Kerringa-Kohn-Rostoker (KKR) condition.

The secular matrix $[P^\alpha(E) - S^\alpha]$ depends on the potential only through the potential functions along the diagonal and for the most localized set it has the TB 2 center form with S^α playing the role of the transfer integrals.

The screened field $|k^0\rangle$ is given by the superposition of bare fields $|k^0\rangle$, and the relationship between the bare and screened structure matrices is;

$$S^\alpha = S^0(1 - S^0)^{-1} \quad (6)$$

The expansion co-efficient S^0 forms a Hermitian matrix which is dimensionless and independent of the scale of the structure. This is a so-called (bare) canonical structure matrix.

The KKR equations have the form of an Eigen value problem if P^α is a linear function of E. This is true if $\alpha = \gamma$ (potential parameter), in which case the effective 2 center Hamiltonian is;

$$H^\gamma_{ij} = C_i S_{ij} + (\sqrt{\Delta_i}) S^\gamma_{ij} (\sqrt{\Delta_i}) \quad (7)$$

For crystals where the matrix inversion in Eq. (7) can be performed, one may obtain from S^0 (or) S^α .

To obtain the Eigen value when $\alpha \neq \gamma$, energy independent orbitals are needed. Now, $|\chi^\alpha(E)\rangle$ is independent of energy, in the interstitial region and in the spheres; its first energy derivative at E_γ will vanish. Therefore, the orbital base is;

$$|\chi^\alpha\rangle = |\phi\rangle + |\phi^\alpha\rangle h^\alpha \quad (8)$$

In this base, the Hamiltonian matrices are;

$$\langle \chi | H - E_\gamma | \chi \rangle = h(1 + oh) \quad (9)$$

$$(H - E) |\phi(E)\rangle = 0 \quad (10)$$

$H - E_\gamma$ is the effective 2 center TB Hamiltonian. This has a shorter range. Therefore, this set of equations is used in self consistent calculations. In the interstitial region, Eq. (9) becomes;

$$\langle \chi^\alpha | H - E_\gamma | \chi^\alpha \rangle = h^\alpha (1 + o^\alpha h^\alpha) \quad (11)$$

The set of $|\chi^\alpha\rangle$ is thus complete to the first order in $(E - E_\gamma)$, and it can yield energy estimates correct to the third order. A Von-Barth and Hedin [12] parameterization scheme has been used for the exchange correlation potential within the Local density approximation (LDA). The accuracy of the total energies obtained within the density functional theory, often using LDA, is in many cases sufficient to predict which structure at a given pressure has the lowest free energy [13]. The atomic sphere approximation (ASA) has been used in the present work. The Wigner-Seitz sphere is chosen in such a way that the sphere boundary potential is at its minimum and the charge flow is in accordance with the electronegativity criteria. s, p and d partial waves are included. The tetrahedron method [14] of the

Brillouin zone (k -space) integration has been used to calculate the density of states. The configurations of Ti 4s², 3d² and H 1s¹ are treated as the valence electrons. Pressure calculations are done with the second order Birch Murnaghan equation of states [15].

$$P = \frac{3}{2} B_0 \left[\left(\frac{V_0}{V} \right)^{7/3} - \left(\frac{V_0}{V} \right)^{5/3} \right] \times \left[1 + \frac{3}{4} (B_0' - 4) \left[\left(\frac{V_0}{V} \right)^{2/3} - 1 \right] \right] \quad (12)$$

where B and B' are the bulk modulus and the first derivative of the bulk modulus respectively.

Results and discussion

Geometric property

At ambient conditions, the Ti, TiH, TiH₂ and TiH₃ crystallize in fcc structure with the space group Fm $\bar{3}$ m (225). The Wyckoff positions for Ti and H atom for TiH are 4a:(0,0,0) and 4b:(0.5,0.5,0.5), and for TiH₂, the Wyckoff positions for Ti and H atom are 4a:(0,0,0) and 8c:(0.25,0.25,0.25), respectively, and contain four formula units per unit cell. The primitive unit cells of Ti, TiH, TiH₂ and TiH₃ are shown in **Figure 1**.

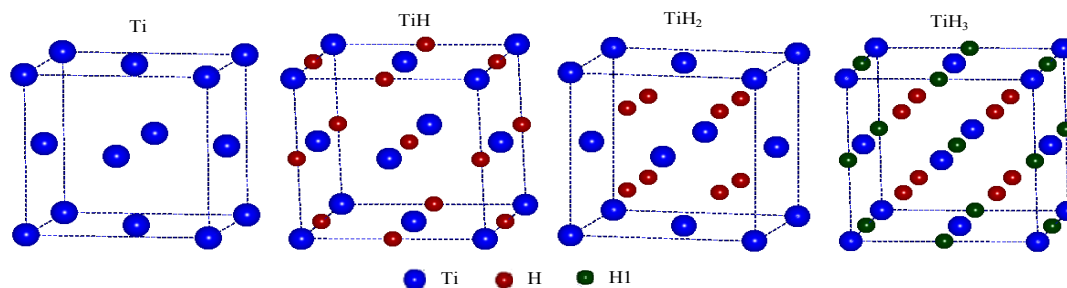


Figure 1 Primitive unit cell of Ti, TiH, TiH₂ and TiH₃.

Valence electron density (VED) is defined as the total number of valence electrons divided by volume per unit cell, which is an important factor for analyzing super hard materials. The equilibrium volume $V_0(\text{\AA}^3)$, optimized lattice parameters $a(\text{\AA})$, $c(\text{\AA})$, total energy (Ry), Density of states (DOS) at the Fermi level $N(E_F)$ (DOS(States/Ry.Cell)), Radius of the Wigner-Seitz cell (R_{wz}), Band Energy E_B (Ry), and Fermi energy E_F (Ry) obtained from the TB-LMTO method are listed in **Table 1**. From this table, it is worth noticing that all VEDs for cubic TiH, TiH₂ and TiH₃ structure are similar to Ti metal (0.2804 electrons/ \AA^3). The equilibrium volumes per f.u for TiH, TiH₂ and TiH₃ structure are higher than that of Ti metal (14.2668 \AA^3) due to the addition of H atoms.

Table 1 Equilibrium volume V_0 (\AA^3), optimized lattice parameters a (\AA), c (\AA), Valence electron density ρ (electrons/ \AA^3), Radius of Wigner-Seitz cell (R_{wz}), Fermi energy E_F (Ry), Band energy E_B (Ry), Density of states (DOS) at the Fermi level $N(E_F)$ (DOS(States/Ry.Cell)) and Total energy $E(\text{total})$ (Ry).

	Ti	TiH		TiH ₂		TiH ₃
	cubic	cubic	hexa	cubic	tetra	cubic
V_0	14.267	17.998	42.741	21.741	42.479	24.810
A	3.85	4.16	3.12	4.388	4.48	4.62
				4.44[Exp. ^a]	4.53[Exp. ^c]	
				4.454[Exp. ^b]	4.486[6]	
				4.428[5]		
C			5.07		4.233	
					4.28[Exp. ^c]	
					4.352[6]	
P	0.2804	0.2778	0.1170	0.2837	0.1412	0.2821
R_{wz}	2.8442	2.4392	2.2564	2.0430	2.1390	2.1546
E_F	0.0418	0.0018	0.0953	0.11602	-0.1707	0.0834
E_B	-0.4286	-1.1846	-1.3958	-1.3440	-2.1870	-2.1141
$N(E_F)$	20.9442	24.9968	44.6083	25.3989	5.1508	30.4820
$E(\text{total})$	-1704.747	-1705.999	-1705.947	-1707.255	-1706.944	-1708.378

^aRef. [16]

^bRef. [17]

^cRef. [18]

The simulated XRD pattern of cubic Ti, TiH, TiH₂ and TiH₃ is shown in **Figure 2**. A monochromatic radiation of wavelength 1.5405 \AA is used to simulate the XRD pattern. The diffraction peaks are obtained using the Lorentz function. The sharp, narrow diffraction peaks show the absence of impurity in the simulated structures. The lattice parameter is calculated using the expression;

$$a = d_{hkl} \times \sqrt{h^2 + k^2 + l^2} \quad (13)$$

The calculated lattice parameter for Ti is 3.85 for all planes (111, 002, 022, 113 and 222), 4.16 \AA for all planes (002, 022, 222 and 004) of TiH, 4.388 \AA for all planes (111, 002, 022, 113, 222, 004 and 133) of TiH₂ and 4.62 \AA for all planes (022 and 004) of TiH₃ which are in good agreement with the available experimental and theoretical data [16-18].

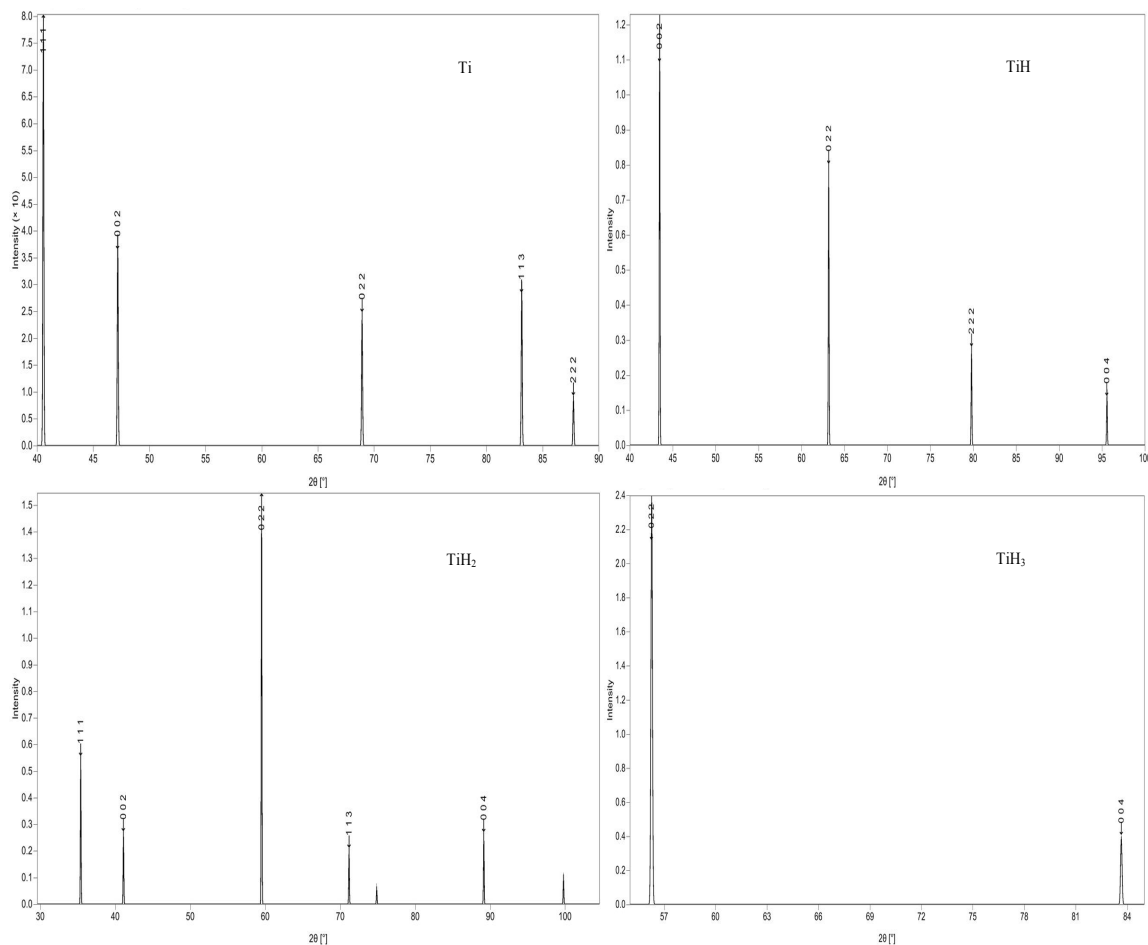


Figure 2 The simulated XRD pattern of cubic Ti, TiH, TiH₂ and TiH₃.

Electronic structure

The band structure of TiH, TiH₂ and TiH₃ is computed for various pressures, and the band structure at normal pressure ($V/V_0 = 1.0$) is given in **Figure 3**. From **Figure 3**, it is seen that, at normal pressure, the band structure has 3 valence bands (bottom most) corresponding to 5 and 6 valence electrons of TiH and TiH₂ which comes from $3d^2 4s^2$ of Ti atom and $1s^2$ state electrons of H atom, and TiH₃ has 4 valence bands corresponding to 7 valence electrons. However, the main hybridization in this energy window concerns the 3d state of Ti atom and s state of hydrogen atom. At the Fermi level, there are overlapping bands which originate from H-1s state and also contain appreciable Ti-3d states. The valence states are separated by a wide gap from the occupied states, indicating covalent behavior. Above the Fermi level, the empty conduction bands are present with a mixed s, p, and d characters. The empty conduction bands are highly overlapping with the valence bands and there is no band gap. Hence, at normal pressure, TiH, TiH₂ and TiH₃ are metals. At high pressure, the bands get dispersed.

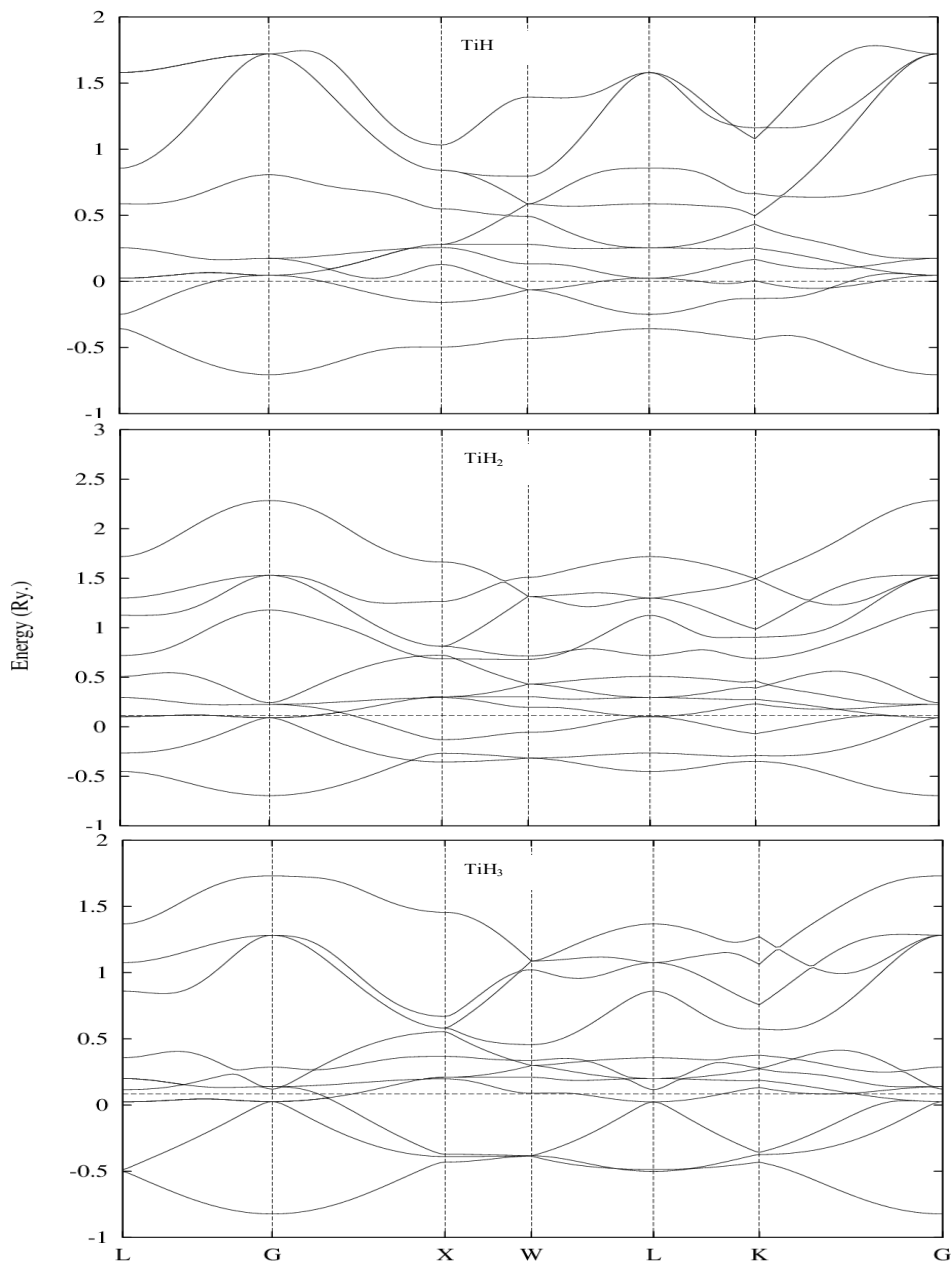


Figure 3 Band structure of cubic TiH and TiH₂ at normal pressure.

To understand the correlation between the electronic and mechanical properties, the density of states under equilibrium geometry has been computed. The total DOS of Ti, TiH, TiH₂ and TiH₃ at normal pressure is shown in **Figure 4**. From **Figure 4**, it is observed that the spike near -0.5 Ry. is due to s state electron of H atom. The highest spike near the Fermi level is due to Ti 3d-like states. The Fermi level is shifted by adding the H atom one by one. As the pressure increases, the height of the spike decreases due to distribution of charge.

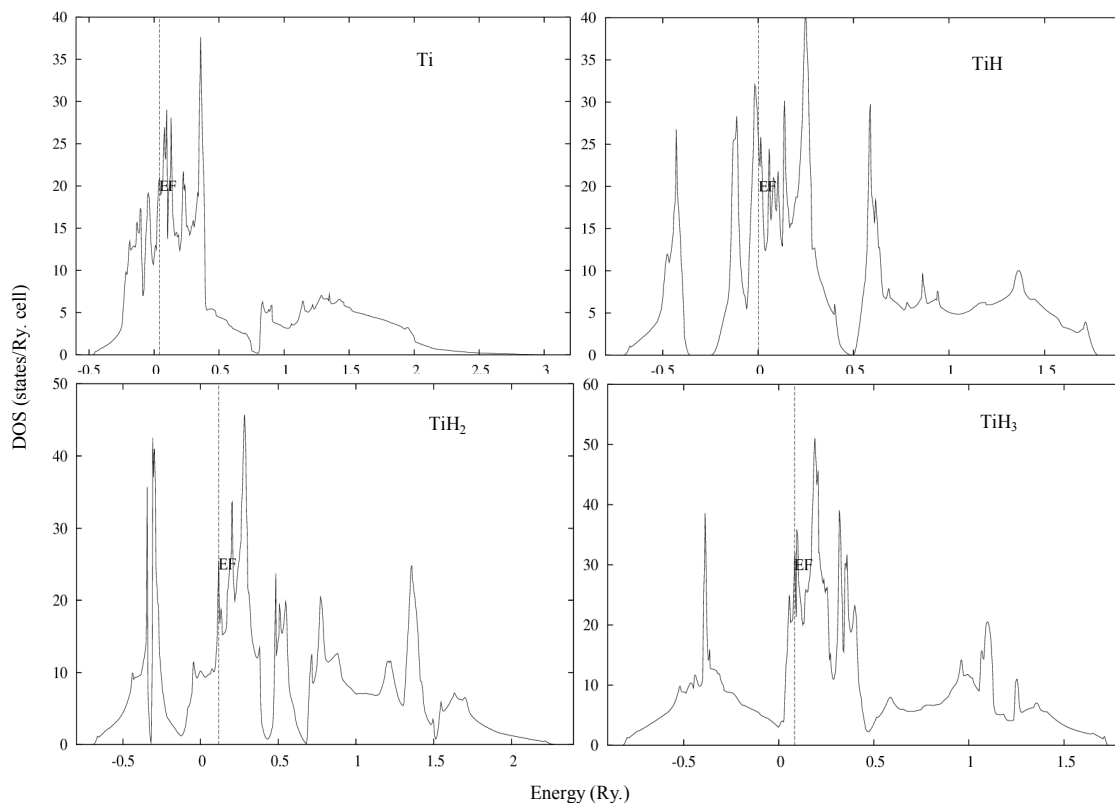


Figure 4 Total density of states of cubic Ti, TiH, TiH₂ and TiH₃ at normal pressure.

Charge density

An understanding of the nature of the chemical bond can be aided by the studies of the distribution of charges in real space. The real space charge density can also be used to understand features of the electronic properties in a real material. One has to remember that the charge density very much depends on the crystal structure, and different characteristics may be formed for one and the same compound in different structural arrangements. The charge density distribution for TiH and TiH₂ are shown in **Figures 5 - 6**. It is clearly seen that charge strongly accumulates between Ti and H atoms, which means that a strong directional bonding exists between them. It is seen that the charge around the Ti site is very much d-like, while that around H site is s-like. Electrons in s, p and d shells of Ti and H at different pressures for cubic TiH₂ are given in **Table 2**. From **Table 2**, it is found that as the pressure increases, a fraction of 4s state electrons are transferred to 4p and 3d states of Ti atom. Similarly, a portion of 1s electrons are transferred to 2p and 3d states of H atom.

Table 2 Electrons in s, p and d shells of Ti and H at different pressures for cubic TiH₂.

Pressure (GPa)	Ti			H		
	4s ²	4p ⁰	3d ²	1s ¹	2p ⁰	3d ⁰
Normal	0.4995	0.7307	2.7293	0.8910	0.1305	0.0190
9.62	0.4841	0.7142	2.7603	0.8902	0.1310	0.0202
22.9	0.4659	0.6904	2.8014	0.8896	0.1306	0.0215
42.0	0.4414	0.6612	2.8577	0.8883	0.1284	0.0230

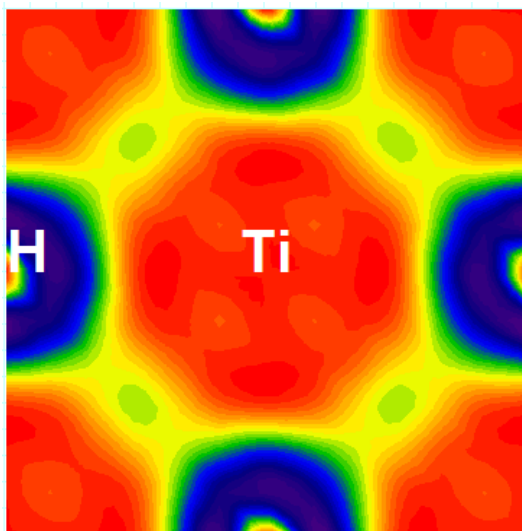


Figure 5 Charge density plot of TiH.

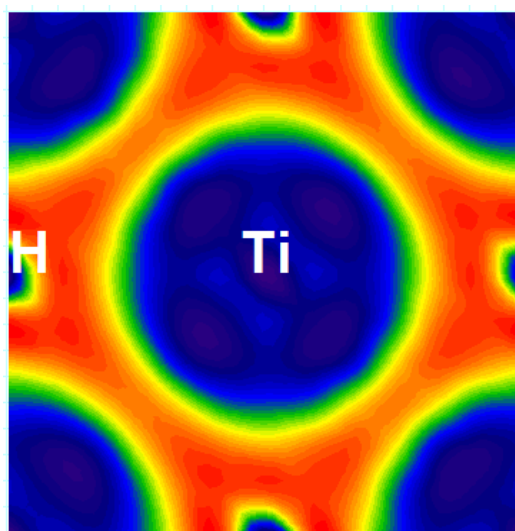


Figure 6 Charge density plot of TiH₂.

Energetics and phase diagram

The structural phase transition in TiH and TiH₂ are studied with the help of total energy calculation. The phase stability is analyzed using the calculated enthalpy values. The enthalpy versus pressure curves corresponding to the 3 different phases of TiH and TiH₂ are shown in **Figures 7 - 8**. From **Figure 7**, it is observed that, at normal and low pressures, the thermodynamically stable phase of TiH is a cubic structure. A pressure induced structural phase transition from cubic to hexagonal phase is observed at a pressure of 15.2 GPa. At high pressure, TiH is stable with a hexagonal phase. From **Figure 8**, it is observed that a structural phase transition from cubic to tetragonal phase occurs at a pressure of 52 GPa. At high pressure, TiH₂ is stable with a tetragonal phase. In order to calculate the transition pressure, the Gibb's free energy is calculated for the 2 phases using the expression;

$$G = E_{\text{tot}} + PV - TS. \tag{14}$$

Since the theoretical calculations are performed at 0 K, the Gibb's free energy will become equal to the enthalpy (H);

$$H = E_{\text{tot}} + PV. \tag{15}$$

At a given pressure, a stable structure is one in which the enthalpy has its lowest value. The transition pressures are calculated at the level at which the enthalpies of the two phases are equal.

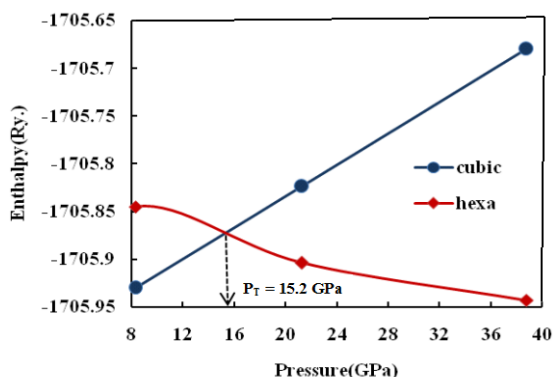


Figure 7 Structural phase transition between cubic and hexagonal phases of TiH.

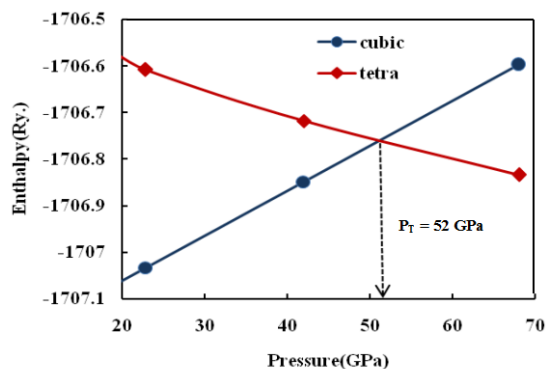


Figure 8 Structural phase transition between cubic and tetragonal phases of TiH₂.

Hydrogen storage in Titanium Hydride

Metal hydrides represent an exciting way of hydrogen storage which is inherently safer than compressed-gas or liquid storage. Also, some intermetallics (including metals and alloys) store hydrogen at a higher volume density than liquid hydrogen. Hydrogen fuel, which can be readily produced from renewable energy sources, contains at least 3 times larger chemical energy per mass 142 MJ Kg than any chemical fuel, thus making hydrogen fuel cells an attractive alternative to the internal combustion engine for transportation. Elements, especially those in group I-IV and some transition metals, have their hydride and amide/imides forms. There is, therefore, still plenty of scope for further exploration of metal-H system for hydrogen storage. In this study, the storage capacity of Ti has been analyzed by adding the hydrogen atom one by one. The formation energy, density of H/unit cell and storage capacity of TiH, TiH₂ and TiH₃ is given in **Table 3**. From the table, it is seen that the formation energy for TiH, TiH₂ and TiH₃ are negative. It shows that the formation is possible. The highest hydrogen storage obtained for TiH₃ is 5.94.

Table 3 Storage capacity of hydrogen in Ti.

	Formation energy	Density of H/unit cell	Weight % of hydrogen
TiH ₁	-0.20	6.51	2.06
TiH ₂	-0.41	11.08	4.04
TiH ₃	-0.48	14.26	5.94

Stability of TiM₂H and TiMH₂

Further, the stability of TiM₂H and TiMH₂ has been studied, where M is the element of 3d transition metals (Sc, V, Cr, Mn, Fe, Co, Ni, Cu and Zn). In order to study the stability of TiM₂H, the heat of formation is calculated from the following relation;

$$\Delta H = E_{\text{tot}}(\text{TiM}_2\text{H}) - E_{\text{tot}}(\text{Ti}) - 2E_{\text{tot}}(\text{M}) - E_{\text{tot}}(\text{H}_2) \quad (16)$$

$$\Delta H = E_{\text{tot}}(\text{TiMH}_2) - E_{\text{tot}}(\text{Ti}) - E_{\text{tot}}(\text{M}) - E_{\text{tot}}(\text{H}_2) \quad (17)$$

where $E_{\text{tot}}(\text{Ti})$, $E_{\text{tot}}(\text{M})$, $E_{\text{tot}}(\text{H}_2)$ are the energies of an isolated titanium, 3d transition metal, and hydrogen atom respectively. $E_{\text{tot}}(\text{TiM}_2\text{H})$ and $E_{\text{tot}}(\text{TiMH}_2)$ are the total energies of the titanium metal hydrides. The calculated value of heat of formation ΔH for mono and dihydrides of titanium with alloying elements of 3d transition metals are shown in **Figures 9 - 10**. From **Figure 9**, it is observed that the 3d transition metals ranging from Mn to Cu in TiM_2H are unstable, and the other titanium metal hydrides are more stable than TiH ($\Delta H = -0.41$ Ry.). From **Figure 10**, it is observed that the stability of TiMH_2 is less than TiH_2 ($\Delta H = -0.48$ Ry.).

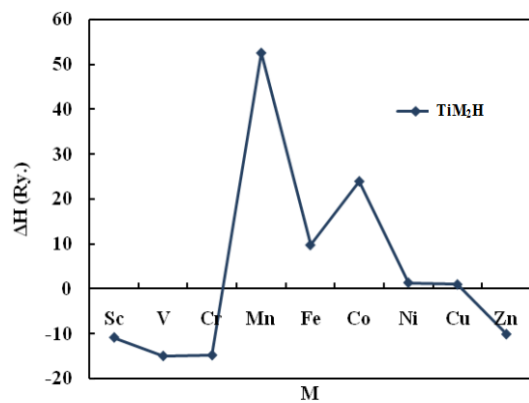


Figure 9 Heat of formation of TiM_2H .

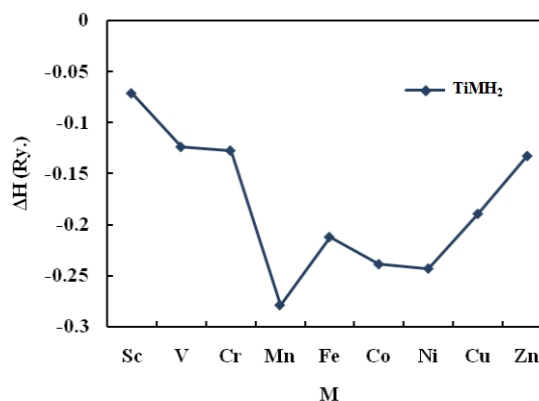


Figure 10 Heat of formation of TiMH_2 .

Conclusions

The band structure, density of states, structural phase transition and charge density under various pressures were investigated based on first principles calculation under the frame work of tight-binding theory within local density approximation. At normal pressure, the thermodynamically stable phase of TiH is NaCl structure and for TiH_2 , CaF_2 phase is more stable. At certain high pressures, the structural phase transition occurs from cubic to hexagonal TiH and cubic to tetragonal TiH_2 phase. Electronic structure calculations show that TiH , TiH_2 and TiH_3 present obvious metallic features. The maximum hydrogen storage capacity achieved was 5.94 % for TiH_3 . The stability of TiM_2H ($\text{M} = \text{Sc}, \text{V}, \text{Cr}, \text{Zn}$) is higher than that of TiH . It is hoped that this work can stimulate further experimental research on Titanium hydride.

Acknowledgement

We thank our college management for their constant encouragement. The financial assistance from UGC (MRP. F.No-38-141/2009), India, is duly acknowledged with thanks.

References

- [1] Y Fukai. *Metal Hydrogen system: Basics Bulk Properties*. Vol I. Springer, Berlin, 2005.
- [2] NL Rosi, J Eckert, M Eddaoudi, DT Vodak, J Kim, M O'Keeffe and OM Yaghi. Hydrogen storage in microporous metal-organic frameworks. *Science* 2003; **300**, 1127-9.
- [3] IP Jain, C Lal and A Jain. Hydrogen storage in Mg: a most promising material. *Int. J. Hydrogen Energy* 2010; **35**, 5133-44.
- [4] MJ Latroche. Structural and thermodynamic properties of metallic hydrides used for energy storage. *J. Phys. Chem. Solids* 2004; **65**, 517-22.
- [5] R Quijano and R de Coss. Electronic structure and energetics of the tetragonal distortion for TiH_2 , ZrH_2 , and HfH_2 : A first-principles study. *Phys. Rev. B* 2009; **80**, 184103-10.

- [6] K Miwa and A Fukumoto. First-principles study on 3d transition-metal dihydrides. *Phys. Rev. B* 2002; **65**, 155114-20.
- [7] VE Antonov. Phase transformations, crystal and magnetic structures of high-pressure hydrides of d-metals. *J. Alloy. Compd.* 2002; **330**, 110-6.
- [8] S Kanagaprabha, AT Asvini Meenaatci, R Rajeswarapalanichamy and K Iyakutti. Electronic structure and magnetic properties of FeH and CoH. *In: Proceeding of the AIP Conference 2012, SRM University, Kattankulathur, Tamilnadu, India, 2012*, p. 71-2.
- [9] S Kanagaprabha, AT Asvini Meenaatci, R Rajeswarapalanichamy and K Iyakutti. First principles study of electronic structure, structural properties and superconductivity of nickel hydride. *Walailak J. Sci. & Tech.* 2012; **9**, 115-26.
- [10] OK Andersen. Linear methods in band theory. *Phys. Rev. B* 1975; **12**, 3060-83.
- [11] HL Skriver. *The LMTO Method*. Vol I. Springer, Heidelberg, 1984.
- [12] U von Barth and L Hedin. A local exchange-correlation potential for the spin polarized case. i. *J. Phys. C Solid State Phys.* 1972; **5**, Article ID 1629.
- [13] NE Christensen, DL Novikov, RE Alonso and CO Rodriguez. Solids under Pressure. Ab Initio Theory. *Phys. Status Solidi B* 1999; **211**, 5-16.
- [14] O Jepsen and OK Andersen. The electronic structure of h.c.p. Ytterbium. *Solid State Commun.* 1971; **9**, 1763-7.
- [15] F Birch. Finite elastic strain of cubic crystals. *Phys. Rev.* 1947; **71**, 809-24.
- [16] WM Mueller, JP Blackledge and GG Libowitz. *Metal Hydrides*. Vol I. Academic Press, New York, 1968.
- [17] HL Yakel. Thermocrystallography of higher hydrides of titanium and zirconium. *Acta Crystallogr.* 1958; **11**, 46-51.
- [18] Y Fukai. *The Metal-Hydrogen System-Basic Bulk Proper-Ties*. Springer Series in Materials Science, Springer, Verlag, Berlin, 1993, p. 1-95.